TECHNICAL MEMORANDUM

NUREG-CR-0741
ANL-CT-79-30

SOME NUMERICAL RESULTS

WITH

THE COMMIX-2 COMPUTER CODE

by

V. L. Shah, J. L. Krazinski, C. C. Miao, and W. T. Sha

Components Technology Division

Prepared for the

U. S. Nuclear Regulatory Commission
Office of Nuclear Regulatory Research
Washington, D.C. 20555

TECHNICAL MEMORANDUM

NUREG-CR-0741
ANL-CT-79-30
R-7

ARGONNE NATIONAL LABORATORY
9700 South Cass Avenue
Argonne, Illinois 60439

SOME NUMERICAL RESULTS

WITH

THE COMMIX-2 COMPUTER CODE

by

V. L. Shah, J. L. Krazinski, C. C. Miao, and W. T. Sha

March 1979

Prepared by

Components Technology Division
Argonne National Laboratory

for the

U. S. Nuclear Regulatory Commission
Office of Nuclear Regulatory Research
Washington, D.C. 20555

Under Interagency Agreement DOE 40-550-75
NRC FIN No. A2045

TABLE OF CONTENTS

ABSTRACT

The computer code COMMIX-2 has been developed for analyzing and designing thermal-hydraulic aspects of nuclear reactor components. The code employs a two-fluid model for solving transient, three-dimensional two-phase (or single phase) nonhomogeneous and nonequilibrium flow conditions.

This report presents numerical results of four problems selected to demonstrate the capabilities of COMMIX-2: (1) transient single-phase flow with heat source; (2) two-phase flow in a vertical tube, where the surface heat flux is sufficiently high that a single-phase liquid emerges as a mixture of liquid and vapor; (3) separation of vapor and liquid; and (4) a high-pressure jet impinging on a vertical plate. The third and fourth problems were selected to demonstrate, respectively, that the code can handle computational difficulties usually encountered in problems with sharp interfaces, and the important role of interfacial mass and momentum exchange.

The numerical results obtained by COMMIX-2 code are very encouraging. It has not only demonstrated the computational capability but has also exhibited the ability of modeling complex phenomena of the jet impingement problem with very simple interfacial drag and evaporation models.

1. INTRODUCTION

During loss of coolant or transient overpower accident situations, boiling of liquid coolant in a reactor core is expected due to high temperatures of fuel pins. The fluid mixture of liquid and vapor, in such circumstances, is nonhomogeneous with both phases being in nonequilibrium thermodynamic states. It is, therefore, desirable to develop a computer code for obtaining numerical solutions of three-dimensional, transient, two-phase (gas-liquid) flow system with nonequilibrium and nonhomogeneous conditions.

Accordingly, we have developed a transient, three-dimensional, two-phase computer code called COMMIX-2. It is an extension of our COMMIX-1 code,[2] which is restricted to single-phase flow.

The present version of COMMIX-2 uses the two-fluid model of Harlow and Amsden [3] to describe the conservation equations of mass, momentum and energy. Consequently, we can analyze a wide spectrum of flow conditions; i.e., from homogeneous and equilibrium to nonhomogeneous and nonequilibrium conditions. The interactions between two fluids are accounted for by incorporating the corresponding terms in all of the conservation equations.

In the finite difference formulation, we use a staggered grid system with central and partial donor cell finite differencing. The formulations are partially implicit. The iterative scheme is similar to the point relaxation technique without linearization developed by Rivard and Torrey [4]. The conservation equations are solved as a boundary value problem in space and an initial value problem in time.

This report presents some of the results of four problems treated by the current version of COMMIX-2:

(1) Transient single-phase flow with heat source;

(2) Two-phase flow with heat flux;

(3) Separation of vapor and liquid; and

(4) High-pressure jet impingement on a vertical wall.

These results confirm the ability of COMMIX-2 to handle transient, three-dimensional two-phase flow conditions.

Section 2 describes the basic field equations for two-phase flow system. Section 3 provides the numerical solution procedure for integrating those field equations. Sections 4, 5, 6, and 7 present the results of the four problems.

2. Two-Phase Governing Equations

2.1 Two-Phase Flow

When a mixture of two phases (liquid and vapor) is in the non-equilibrium and nonhomogeneous state, transfer of mass momentum and energy between the two phases occurs at the interface. This interaction is a very complex phenomenon and is not well understood. There are several mathematical models in the open literature which postulate the interaction betwen the two phases; consequently, there are several formulations which describe the governing conservation equations.

The current version of COMMIX-2 uses the two-fluid model of Harlow and Amsden. In this model, separate conservation equations are formulated for each phase, and the interaction between the phases is accounted for by including evaporation (or condensation), interfacial drag and interfacial heat transfer terms in the corresponding mass, momentum, and energy equations, respectively. The code, therefore, solves the two-continuity, six-momentum, and four-energy conservation equations and the required thermodynamic constitutive relations.

2.2 Governing Equations

The field equations for the two-fluid model are:

(1) Mass Conservation:

$$\frac{\partial(\theta_\ell \rho_\ell)}{\partial t} + \nabla \cdot (\theta_\ell \rho_\ell \vec{U}_\ell) = \Gamma_\ell \tag{2.1}$$

for the liquid phase, and

$$\frac{\partial(\theta_\ell \rho_\ell)}{\partial t} + \nabla \cdot (\theta_g \rho_g \vec{U}_g) = \Gamma_g = -\Gamma_\ell \tag{2.2}$$

for the vapor phase.

(2) Momentum Conservation:

$$\frac{\partial(\theta_\ell \rho_\ell \vec{U}_\ell)}{\partial t} + \nabla \cdot (\theta_\ell \rho_\ell \vec{U}_\ell \vec{U}_\ell) = -\theta_\ell \nabla P + \nabla \cdot (\theta_\ell \vec{\sigma}_\ell) + \vec{S}_{m\ell} + \theta_\ell \rho_\ell \vec{G} + K(\vec{U}_\ell - \vec{U}_g) \tag{2.3}$$

for the liquid phase, and

$$\frac{\partial(\theta_g \rho_g \vec{U}_g)}{\partial t} + \nabla \cdot (\theta_g \rho_g \vec{U}_g \vec{U}_g) = -\theta_g \nabla P + \nabla \cdot (\theta_g \bar{\sigma}_g) + \vec{S}_{mg} + \theta_g \rho_g \vec{G} + K(\vec{U}_g - \vec{U}_\ell) \quad (2.4)$$

for the vapor phase.

(3) Energy Conservation:

$$\frac{\partial(\theta_\ell \rho_\ell H_\ell)}{\partial t} + \nabla \cdot (\theta_\ell \rho_\ell H_\ell \vec{U}_\ell) = \theta_\ell \frac{\partial P}{\partial t} + \vec{U}_\ell \cdot \nabla P + \Gamma_\ell H_g + R_\ell (T_g - T_\ell) + \Phi_\ell + \nabla \cdot (K_\ell \theta_\ell \nabla T_\ell) + Q_\ell \quad (2.5)$$

for the liquid phase, and

$$\frac{\partial(\theta_g \rho_g H_g)}{\partial t} + \nabla \cdot (\theta_g \rho_g H_g \vec{U}_g) = \theta_g \frac{\partial P}{\partial t} + \bar{U}_g \cdot \nabla P + \left(K + \frac{\Gamma_g}{2}\right)(\vec{U}_g - \vec{U}_\ell)^2 + Q_g + \Gamma_g H_g + R_g (T_\ell - T_g) + \Phi_g + \nabla \cdot (K_g \theta_g \nabla T_g) \quad (2.6)$$

for the vapor phase.

In the foregoing equations, ρ is the density, p is the pressure, H is the enthalpy, and θ is the void fraction, and the subscripts ℓ and g denote the liquid and gaseous phases, respectively. The velocity vector $\vec{U} = u\vec{i} + v\vec{j} + w\vec{k}$, where u, v and w represent the velocity components in x, y and z directions respectively. Γ_ℓ and Γ_g are the volumetric source terms in the continuity equations due to condensation or evaporation. In the momentum equation $\vec{G}$ is the gravitational body force, K is the interfacial drag coefficient, S_m is the momentum transfer due to mass transfer at the interface, and $\bar{\sigma}$ is the viscous stress tensor. Similarly, in the energy equation, R is the interfacial heat transfer coefficient, k is the thermal conductivity, Φ is the viscous dissipation term, and Q is the heat source. We have assumed that all energy due to mass transfer and momentum transfer at the interface enters the gaseous phase only. For a two-phase flow, we have

$$\theta_\ell + \theta_g = 1 \quad (2.8)$$

The derivation of the quasi-continuum governing equations is described in Appendix A.

In the present formulation, we have two-mass, six-momentum, and two-energy equations. These equations are solved for θ_ℓ (or θ_g), pressure p, six velocities, and two enthalpies. The densities and temperatures are obtained through the use of the equations of state.

3. Numerical Procedure

3.1 Formulation

The partial differential equations in Section 2 are solved using the finite difference procedure. We use a staggered grid system to differentiate between the field and flow variables. Thus we define field variables (p, ρ, θ, H, T) at the center of a cell, and flow variables (u, v, w) at the surface of a cell. The finite difference equations are formulated using the partial donor cell differencing scheme for all convective fluxes, and central differencing scheme for the rest of the terms. Except for the convective and diffusion terms, the variables in all terms are defined at new time variables. Therefore, the formulations are partially implicit and consequently requires an iterative solution procedure.

3.2 Iterative Scheme

The finite difference equations of mass, momentum, and energy are solved as an initial value problem in time and boundary value problem in space. The procedure is iterative and the main steps necessary to determine the flow conditions at time $t + \Delta t$ from those at time t are as follows:

(1) The pressure distribution at time $t + \Delta t$ is estimated.

(2) The momentum equations are solved to yield a first approximation of the three velocity components of each of the two phases.

(3) Partial energy equations are solved for approximating enthalpies of both phases.

(4) Densities and temperatures of both phases are calculated using equation of state and estimated enthalpies and pressures.

(5) Liquid void fraction θ_ℓ is estimated from the continuity equation of liquid. Gas void fraction θ_g is then calculated from the relation $\theta_g = 1 - \theta_\ell$.

(6) The gas continuity equation is now checked if it is satisfied. If the equation is not satisfied, the pressure is corrected, the amount of correction being dependent on the mass residual. Steps (2) to (6) are then repeated. This iterative procedure is continued until the mass residual is less than the prespecified value.

(7) Energy equations are solved for enthalpies. Temperatures and densities are then calculated using the equations of state.

(8) A new time step is chosen and steps (1) to (7) are repeated.

4. Single Phase Flow With Uniform Heat Source

4.1 Problem

At time t=0, a horizontal duct (open at both ends) contains air at constant pressure with zero velocity. Due to uniform heat source and constant outlet pressure boundary conditions, air begins to move and an oscillatory type pressure distribution is created inside the duct. The schematic layout is shown in Fig. 4.1.

This problem was selected to enable a comparison of numerical results with the following analytical solution. The transient pressure distribution for a one-dimensional compressible flow problem with uniform heat generation is given by

$$p(t,x) = p_o e^{y(t,x)} \quad . \tag{4.1}$$

where

$$y(t,x) = \frac{2aL}{c_0} \sum_{n=1}^{\infty} \frac{[1+(-1)^{n+1}][Y_0(z_0)J_0(z) - J_0(z_0)Y_0(z)]}{n^2\pi^2[Y_0(z_0)J_1(z_0) - Y_1(z_0)J_0(z_0)]} \sin \frac{n\pi x}{L}, \tag{4.2}$$

$$Z = -\frac{2}{a}\frac{n\pi}{L} c_0 \bar{e} \frac{at}{2}, \tag{4.3}$$

$$c^2 = p/\rho, \tag{4.4}$$

Y_0, Y_1, Z_0, Z_1 are the Bessel functions, and the subscript 0 is for time t = 0.

4.2 Results

Figure 4.2 shows the transient pressure fluctuati. at the center plane of the duct. We can see that our numerical results are in close agreement with the analytical solution.

5. Two-Phase Flow in a Vertical Tube

5.1 Problem

The schematic layout is shown in Fig. 5.1, and the geometric and input parameters are given below:

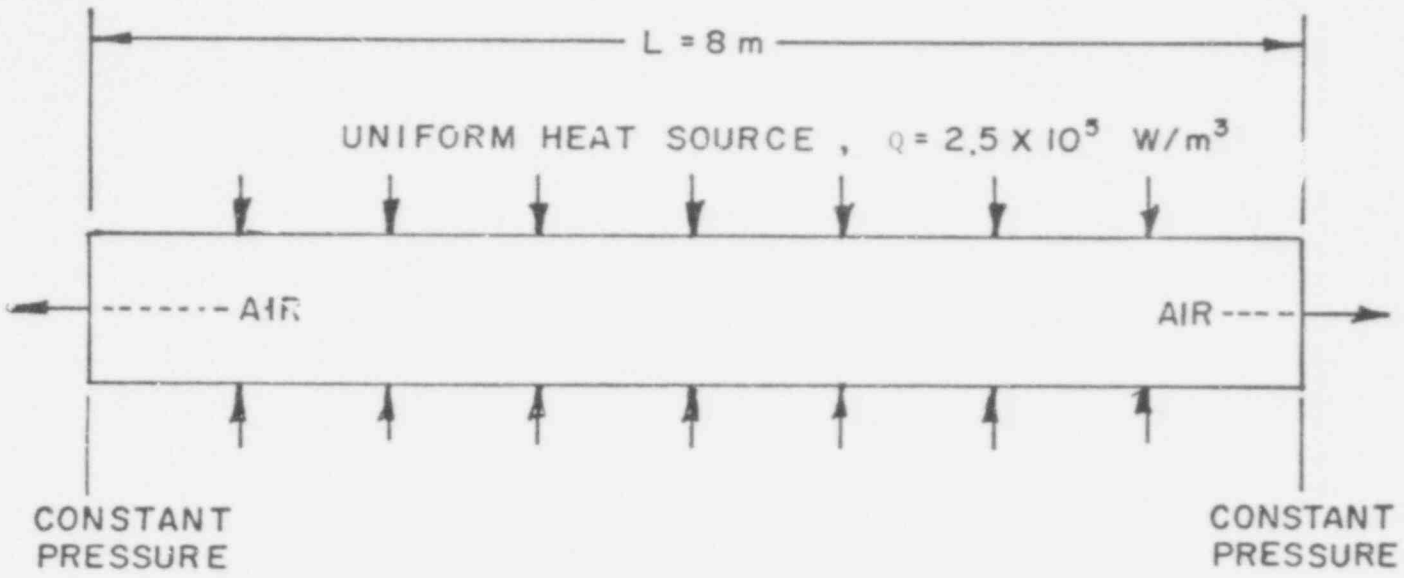

Fig. 4.1. Duct With Uniform Heating

(Initial Pressure = 1 atm.; Boundry Pressure = 1 atm)

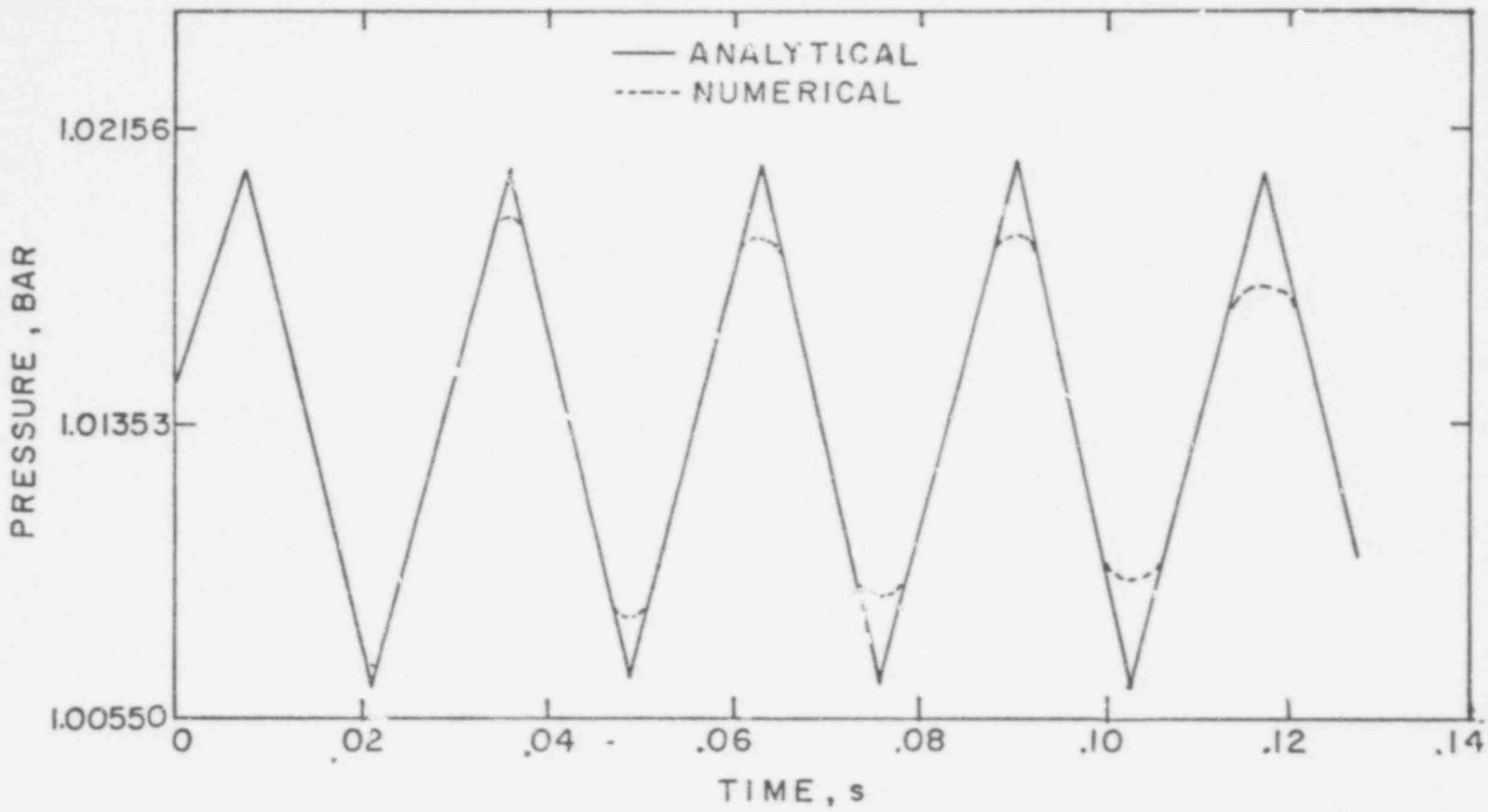

Fig. 4.2. Variation of Pressure at the Central Plane Due to Uniform Heating

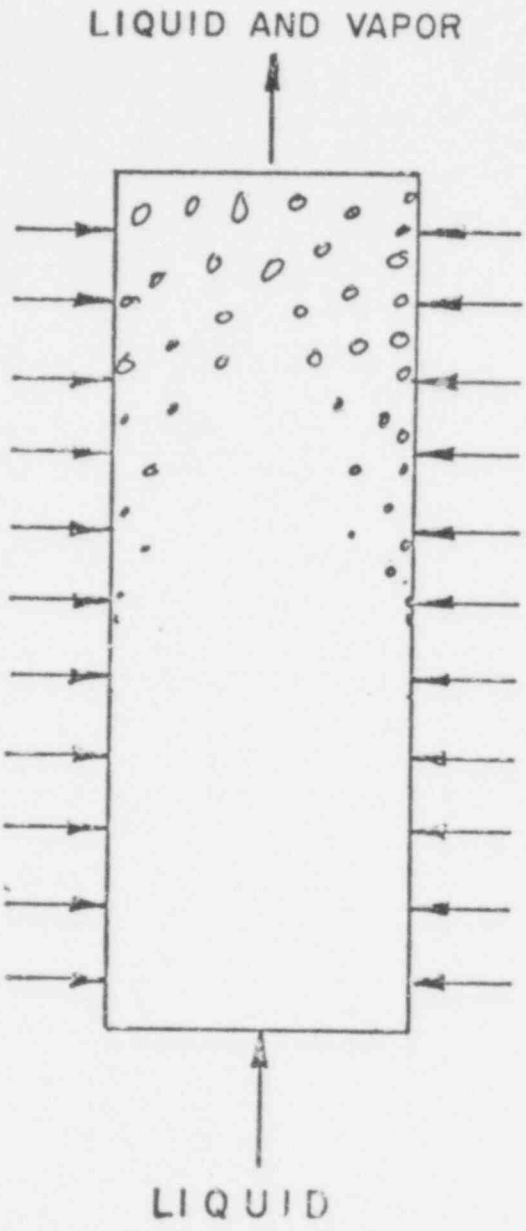

Fig. 5.1. Vertical Duct with Surface Heat Flux.

Geometry: 0.1 m x 0.1 m x 0.9 m long square duct

Inlet Temp: 99.75°C

Inlet Pressure: 1 atm

Inlet Velocity: 1 m/s

Surface Heat Flux = 5.375×10^4 W/m^2

Fluid = H_2O

To obtain the homogeneous-equilibrium flow conditions, very large values of the interface friction and interface heat transfer parameters were prescribed during computation. The evaporation rate was computed from excess liquid enthalpy over liquid saturation enthalpy.

5.2 Results

The steady-state numerical results are shown in Figure 5.2 and 5.3. The comparison with the theoretical overall energy balance shows that the numerical results are very close to the theoretical steady state solution.

We observed in this problem that numerical results do not converge for high heat flux case due to high rate of vapor generator. On the other hand, for very low heat flux case, we face the problems of round of errors. In order to obtain a good, stable and converging solution, the entire problem was run in double precision on IBM 370.

6. Separation of Steam and Water

6.1 Problem

At time t = 0, we have an isothermal uniform mixture of steam and water in a rectangular vertical closed duct. As time proceeds, due to gravity, vapor starts moving up and liquid starts moving down. The separation continues until all vapor occupies the upper section of the duct and all liquid occupies the lower part of the duct.

6.2 Results

To determine the effect of interfacial drag on separation, we have carried out numerical computation for interfacial drag coefficient K = 10^3, 10^4, and 10^5 kg/m^3·s. Figure 6.1 shows the liquid particle distribution at various time steps. Figure 6.2 shows the variation of void fraction with time in the top and the bottom cells of the vertical duct. The rate of separation increases as interfacial drag coefficient decreases. Figure 6.3 shows the transient variation of void fraction in the duct.

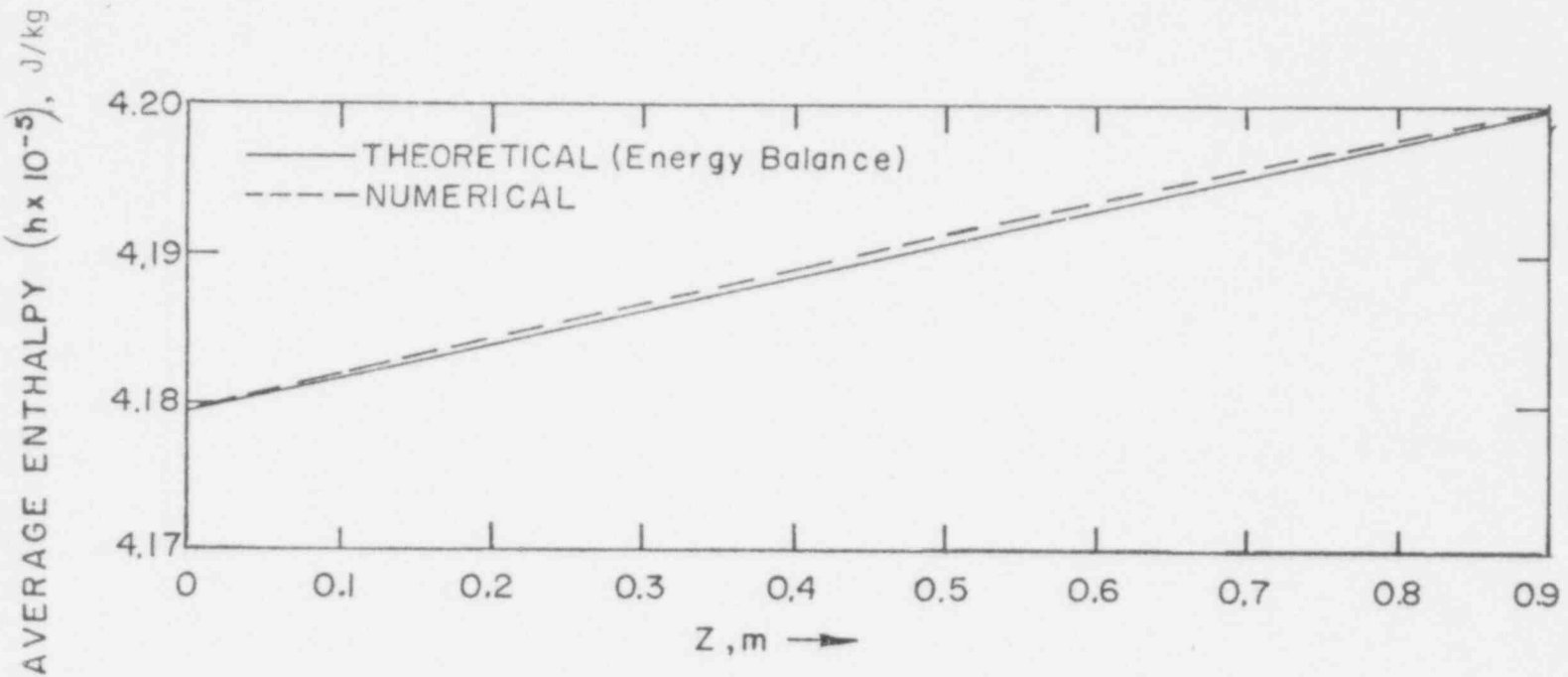

Fig. 5.2. Enthalpy Distribution in a Vertical Heated Duct.

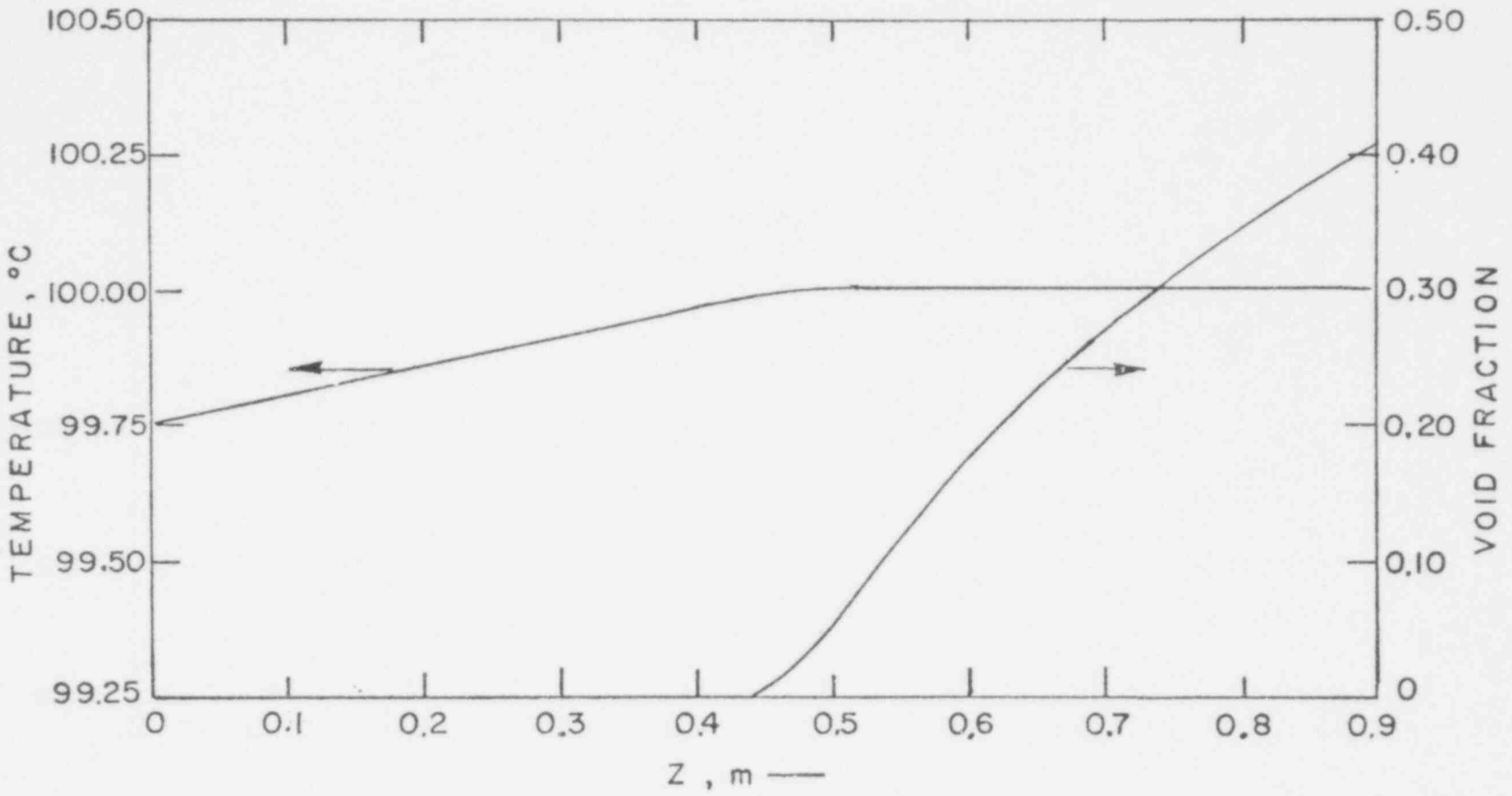

Fig. 5.3. Variation of Temperature and Void Fraction in a Vertical Heated Duct

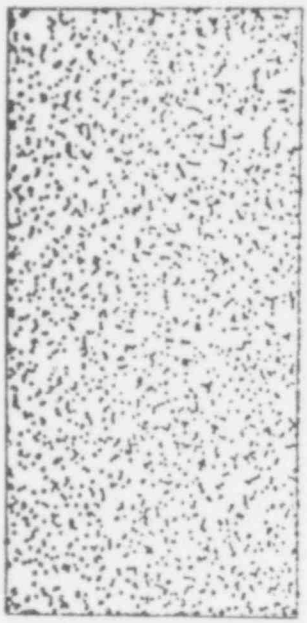

0.0000

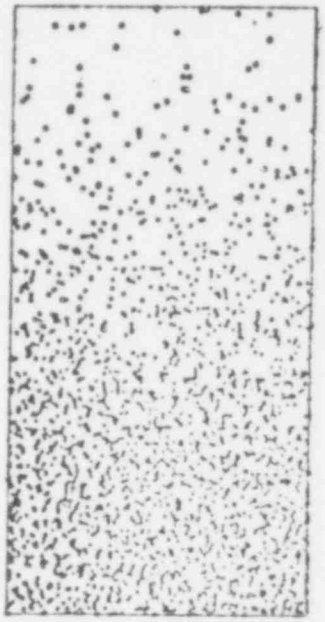

0.1701

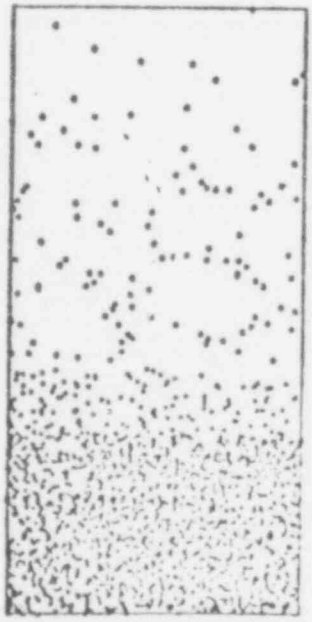

0.6231

0.8001

Fig. 6.1. Distribution of liquid particles at t = 0, 0.1701, 0.6231, and 0.8001 s.

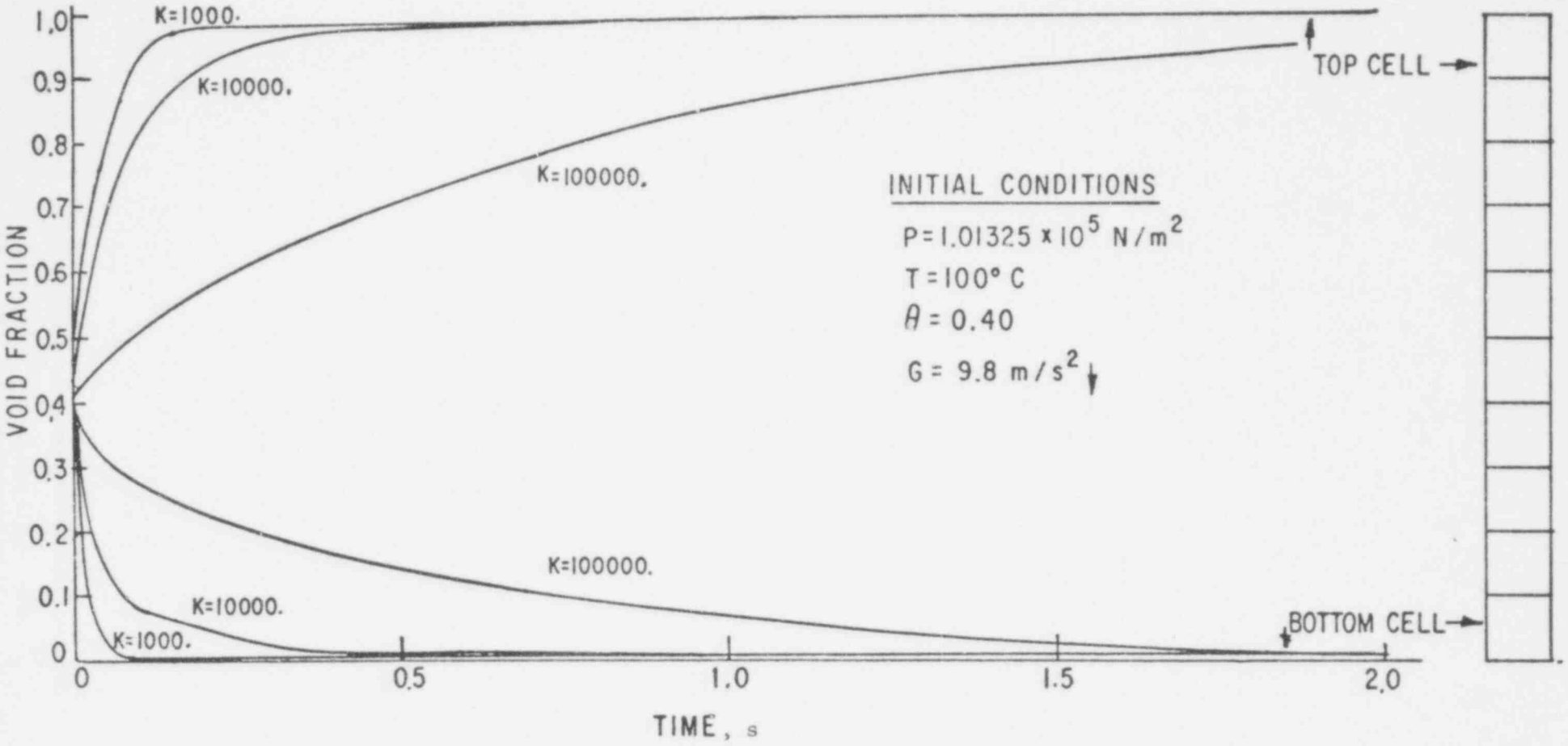

Fig. 6.2. Effect of Interfacial Drag Coefficient K on the Variations of Void Fraction in Top and Bottom Cells

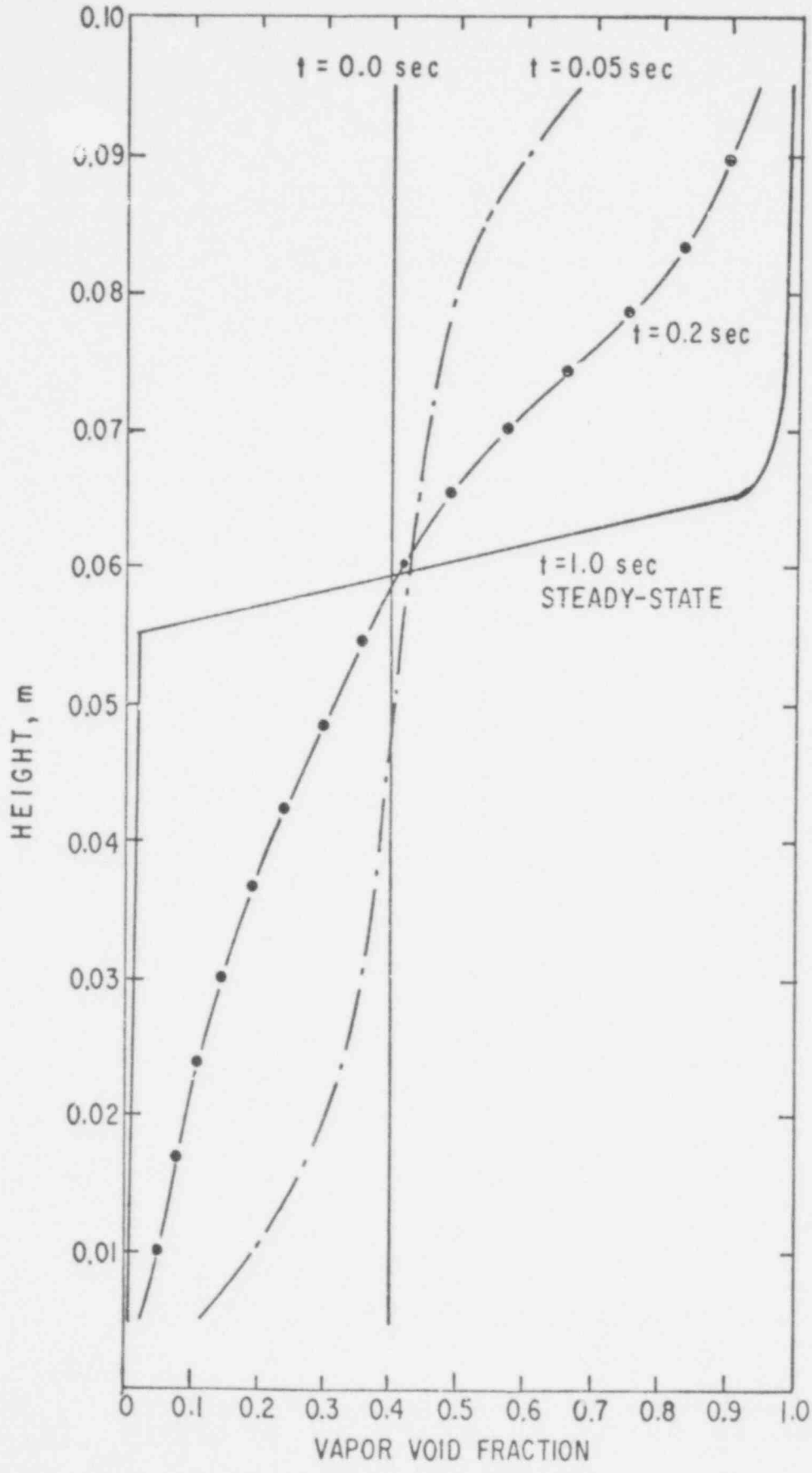

Fig. 6.3. Variation of Void Fraction with Time for Drag Coefficient $K = 10^4$.

There are no experimental measurements available to verify the computed values. However, the trends are typical of the behavior expected in a real physical situation.

7. High Pressure Jet Impingement

7.1 Problem

At time t = 0, a high-pressure jet containing a mixture of steam (67%) and water (33%) enters into a stagnant atmosphere and impinges on a vertical wall. The schematic layout is shown in Fig. 7.1.

This two-phase problem was selected for the following reasons:

(1) The high-pressure liquid jet expands as it leaves the nozzle. Due to expansion, some of the liquid evaporates. The problem, therefore, involves a source term in the continuity equation.

(2) Experimental measurements [5] for a steady-state case are available for verification of our numerical results.

The axial velocity and pressure distributions at the mid-plane between the exit of nozzle and the impinged wall are shown in Figs. 7.2 and 7.3. As time proceeds, the velocity and pressure increase, reach maximum values at $t = 3.5 \times 10^{-5}$ s, and thereafter decrease to steady-state values. Figure 7.4 shows the velocity profile at various axial positions z for $t = 7.2 \times 10^{-5}$ s, where z is the distance from the exit of the nozzle.

Figures 7.5 and 7.6 present comparisons between COMMIX-2 calculations and steady-state pressure measurements on the impinged wall, and corresponding sensitivity study of variations of interfacial drag coefficient (K) and evaporation rate (Γ_g). There is good agreement between experimental data on pressure distribution and the calculated results for $K = 2.0 \times 10^{12}$ kg/m^3·s, and $\Gamma_g = 0.1$ kg/m^3·s.

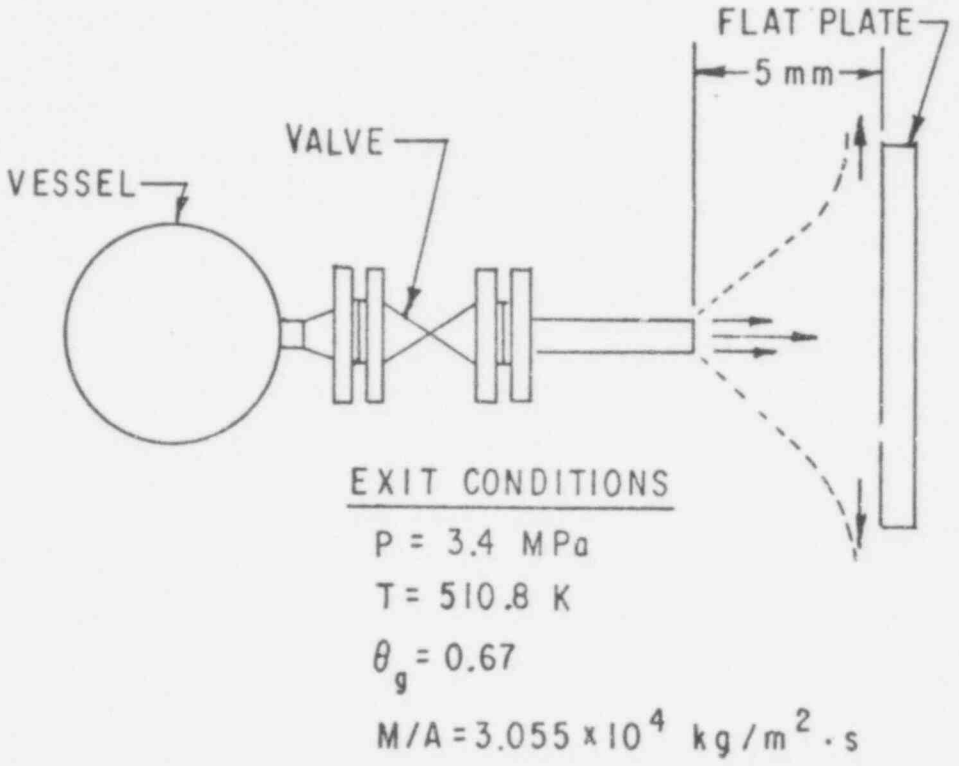

Fig. 7.1. Schematic of Two-Phase Jet Impingement Experiment

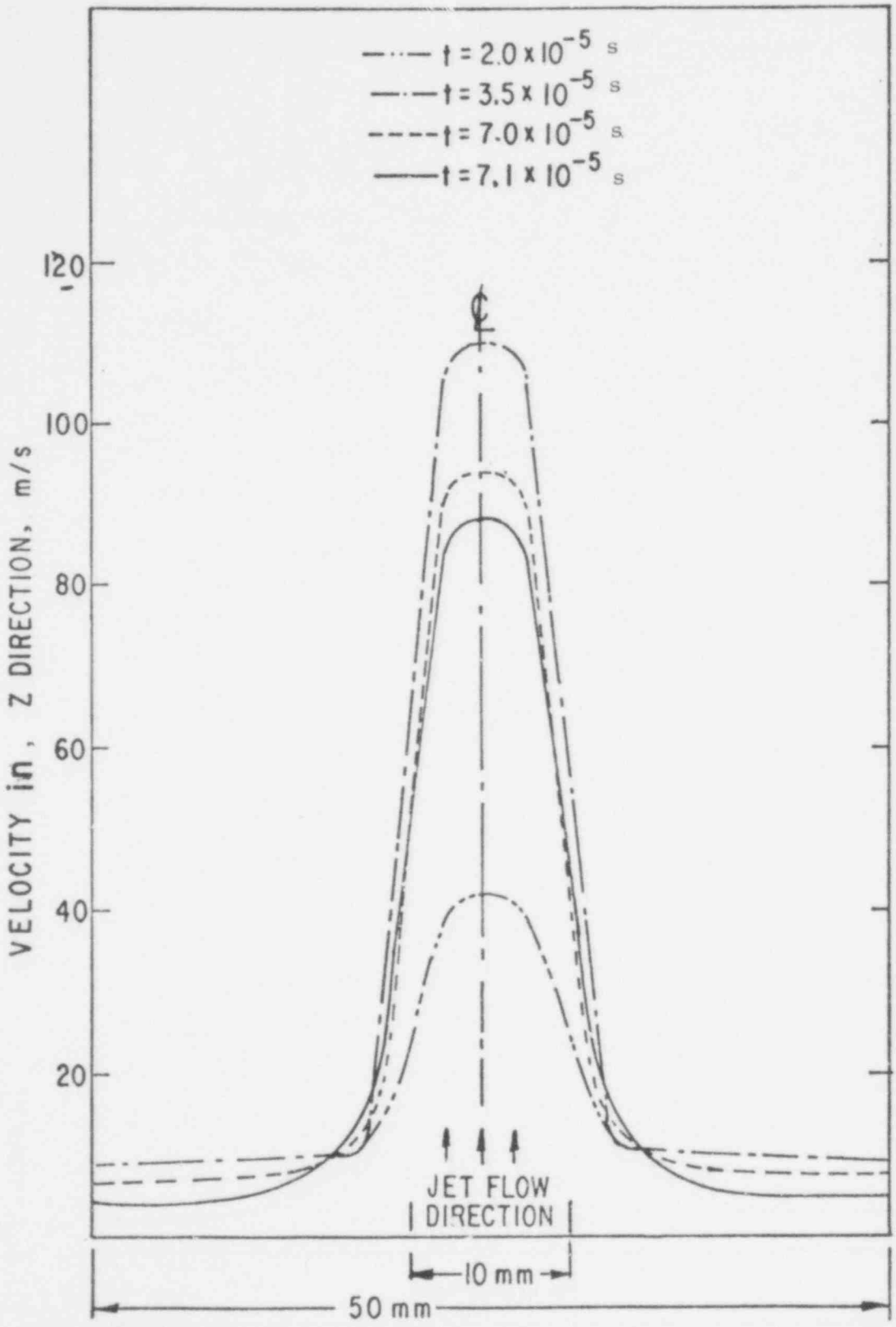

Fig. 7.2. Variation of Velocity Distribution at Mid-Plane Between the Exit of Nozzle and the Impinged Wall (Γ_g = 0.1 kg/m^3·s; K = 2.0 x 10^{12} kg/m^3·s).

466 065

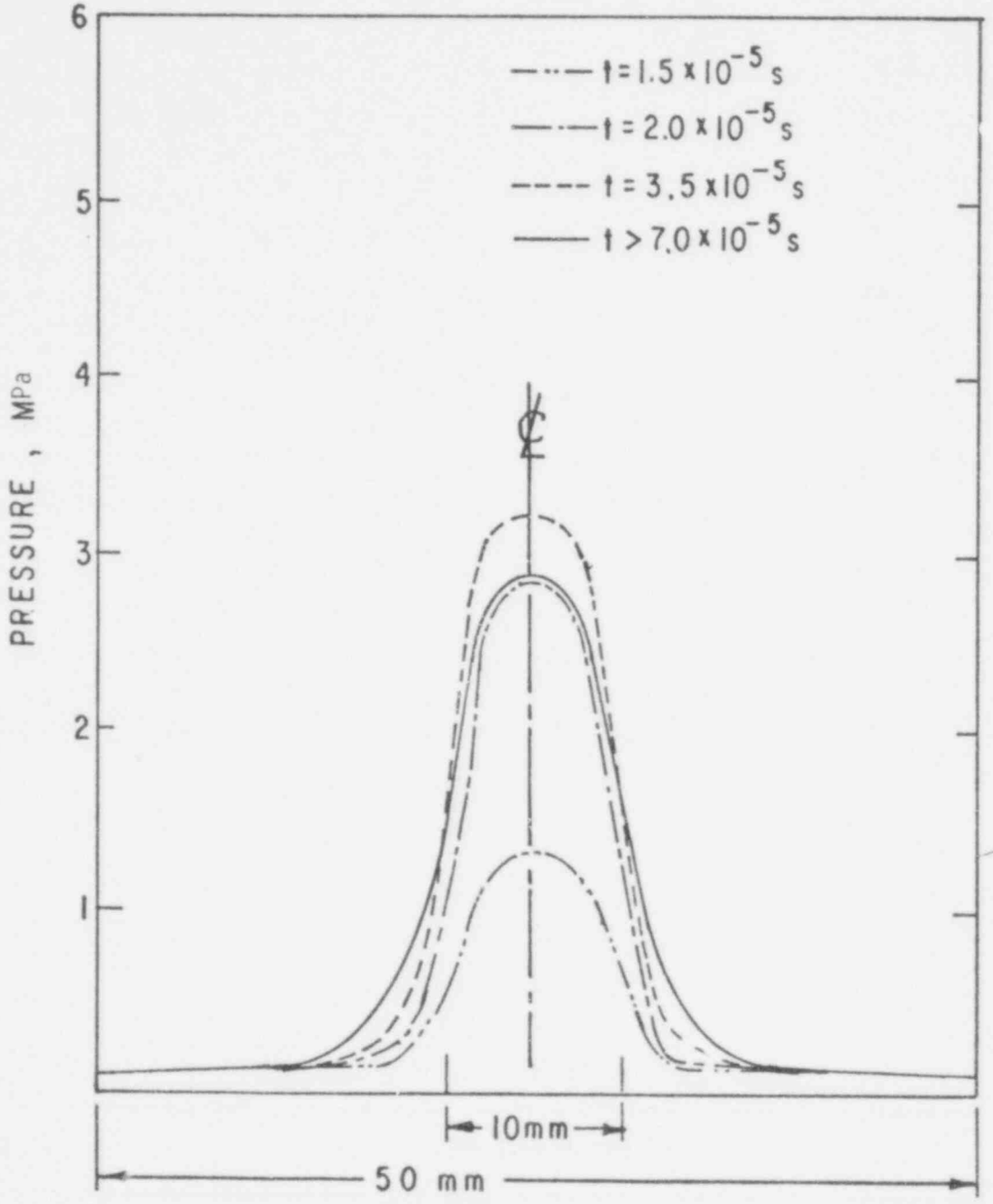

Fig. 7.3. Variation of Pressure at Mid-Plane Between the Exit of Nozzle and the Impinged Wall (Γ_g = 0.1 kg/m^3·s; K = 2.0 x 10^{12} kg/m^3·s).

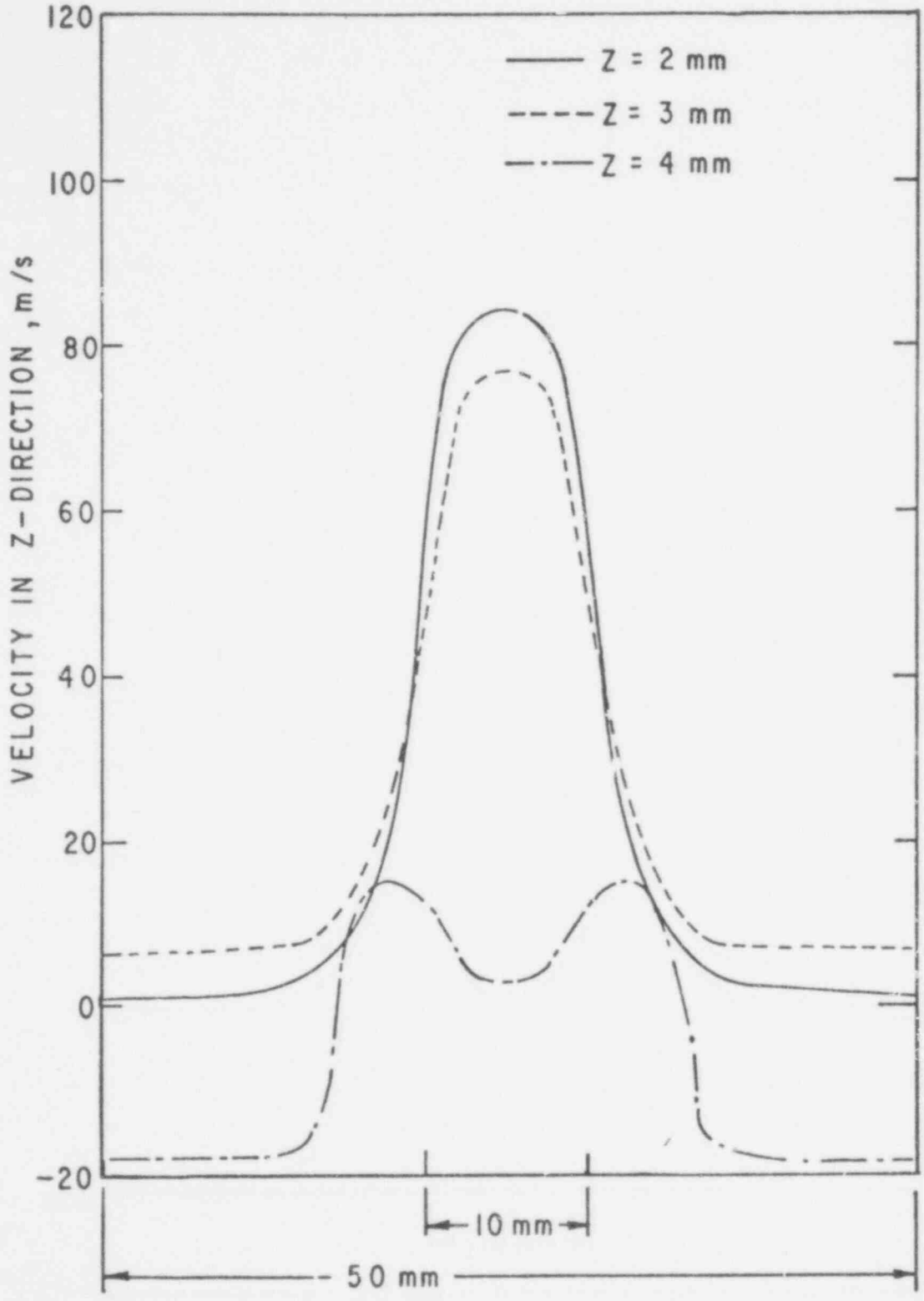

Fig. 7.4. Velocity Profiles at Various Axial Positions for $t = 7.20 \times 10^{-5}$ s; $\Gamma_g = 0.1$ kg/m^3·s, and $K = 2.0 \times 10^{12}$ kg/m^3·s.

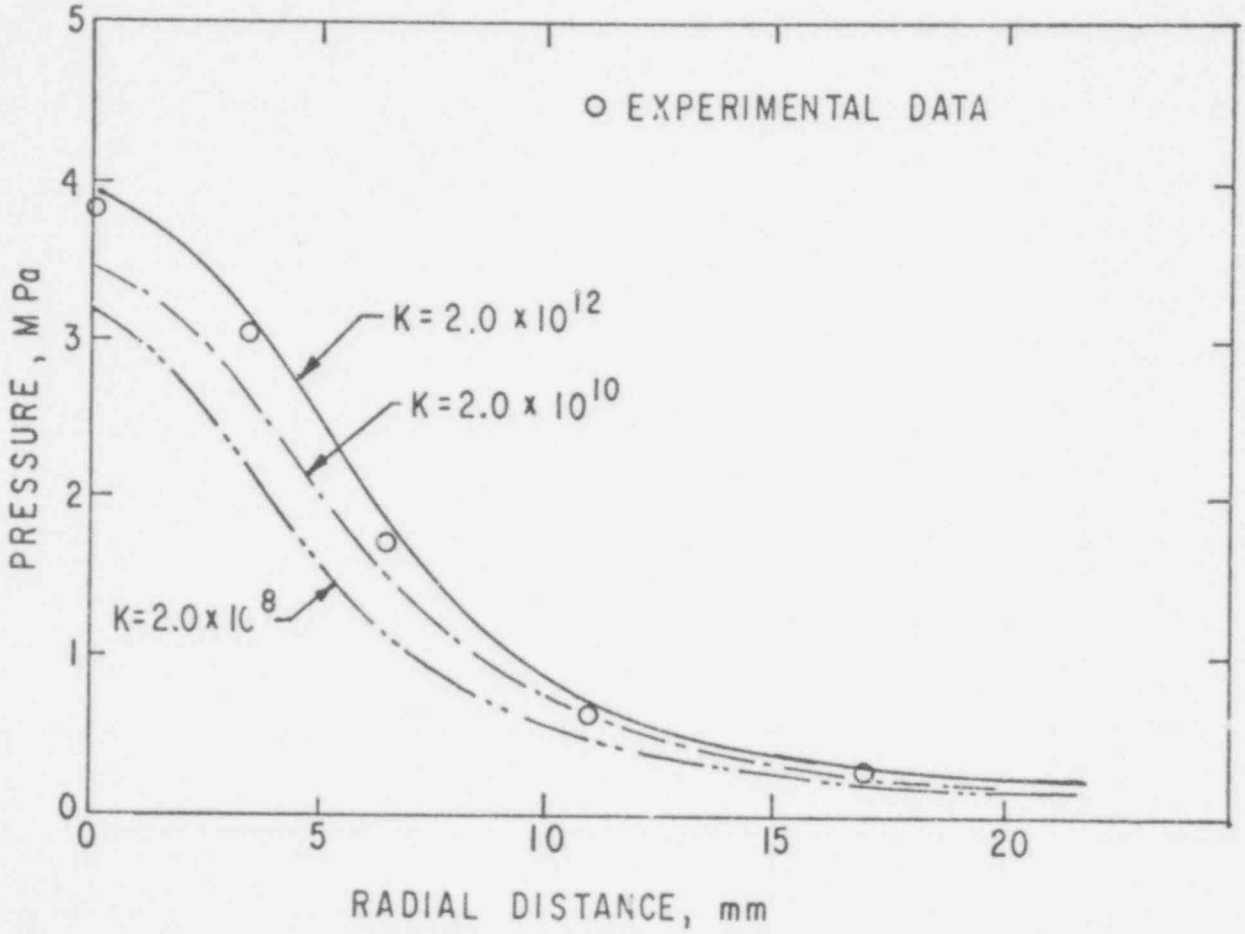

Fig. 7.5. Effect of K on Steady-State Pressure Distribution Over the Impinged Wall (Γ_g = 0.1 kg/m^3·s).

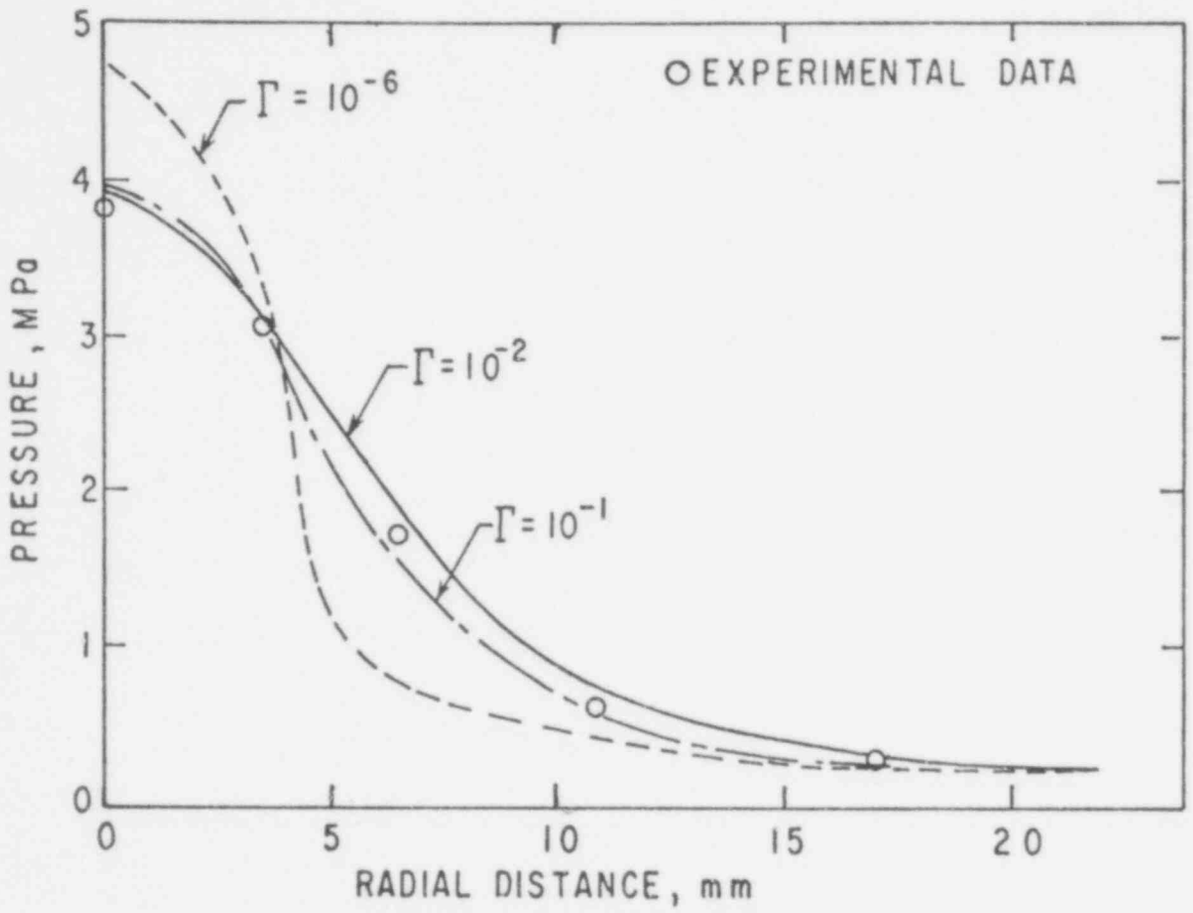

Fig. 7.6. Effects of Evaporation Rate on Steady-State Pressure Distribution Over the Impinged Wall (K - 2.0 x 10^{12} kg/m^3·s).

ACKNOWLEDGEMENTS

We are indebted to R. C. Schmitt and Dr. W. H. Lee for their help during the initial stages of the development of the computer program; to Mrs. S. A. Moll and Mrs. K. M. Mowery for typing the manuscript, and to Drs. R. T. Curtis, C. N. Kelber, and P. M. Wood of the United States Nuclear Regulatory Commission, for their support, without which this work would not have been possible.

Appendix A

DERIVATION OF QUASI-CONTINUUM GOVERNING EQUATIONS FOR TWO-PHASE FLOW

A.1 Introduction

In this appendix, a set of quasi-continuum governing equations for conservation of mass, momentum, and energy is derived. These equations are applicable to a class of systems, such as heat exchangers and fuel rod bundles, wherein the flow domain contains numerous dispersed solid objects.

The presence of solid objects in a flow domain has two effects on fluid flow. One is the geometrical effect; here, the presence of solid objects influences the flow by reducing the available space. We take this effect into account by including the surface and volume porosities in the governing equations. The second effect is the physical effect; here, the solid objects influence the momentum and heat transfer to fluid flow. This we take into account by considering solid objects within a control volume as distributed resistances to momentum transfer and distributed sources (or sinks) for heat transfer.

Although we have considered here only a two-phase (liquid-gas) system, the formulations can be extended easily for application to a multiphase system.

A.2 Assumptions

In deriving the set of quasi-continuum governing equations we have made the following assumption:

> A real system containing numerous solid objects can be replaced by an idealized system having uniformly distributed solid objects such that both systems have the same volumetric porosities, surface permeabilities, and interactions (momentum and heat transfer) between fluid and solid surfaces.

A.3 Volume Porosity and Surface Permeability

Consider a stationary volume element $\Delta x\Delta y\Delta z$ through which fluid is flowing (see Fig. A.1). The total volume

$$\Delta V = \Delta x\Delta y\Delta z = \Delta V_f + \Delta V_s, \tag{A.1}$$

where ΔV_f is the volume occupied by fluid, and ΔV_s is the volume occupied by all solid objects. We define the volume porosity γ_v as the ratio of the volume occupied by fluid to the total volume; i.e.,

$$\gamma_v = \Delta V_f/(\Delta V_f + \Delta V_s) = \Delta V_f/(\Delta x\Delta y\Delta z). \tag{A.2}$$

The surface permeability is defined as the ratio of surface area through which fluid is flowing, to the total cross-sectional area. Thus, for a surface permeability in the x-direction (see Fig. A.2),

$$\gamma_x = \frac{\left(\int_0^{\Delta z} \int_0^{\Delta y} dy\, dz \right)}{(\Delta y \Delta z)} \text{ fluid surface.} \tag{A.3}$$

The surface permeabilities in the y- and z-directions are similarly defined.

A.4 Continuity Equation

Consider the mass balance of phase i (i = 1 or 2) over a stationary volume element $\Delta x \Delta y \Delta z$ through which the fluid is flowing (see Fig. A.3). Let θ_i represent the fraction of fluid volume occupied by phase i, and Γ_i the source of phase i per unit volume occupied by fluid. The mass balance can be written as:

$$\begin{aligned}
\frac{\partial}{\partial t}(\rho_i \theta_i \gamma_v \Delta x \Delta y \Delta z) = {} & \left(\rho_i \theta_i u_i \gamma_x \Delta y \Delta z\right)_{x-\frac{\Delta x}{2}} - \left(\rho_i \theta_i u_i \gamma_x \Delta y \Delta z\right)_{x+\frac{\Delta x}{2}} \\
& \text{(Rate of change)} \qquad \text{(flux in x-direction)} \\
& + \left(\rho_i \theta_i v_i \gamma_y \Delta x \Delta z\right)_{y-\frac{\Delta y}{2}} - \left(\rho_i \theta_i v_i \gamma_y \Delta x \Delta z\right)_{y+\frac{\Delta y}{2}} \\
& \qquad \text{(flux in y-direction)} \\
& + \left(\rho_i \theta_i w_i \gamma_z \Delta x \Delta y\right)_{z-\frac{\Delta z}{2}} - \left(\rho_i \theta_i w_i \gamma_z \Delta x \Delta y\right)_{z+\frac{\Delta z}{2}} \\
& \qquad \text{(flux in z-direction)} \\
& + \Gamma_i \gamma_v \Delta x \Delta y \Delta z \quad \text{(source)} ,
\end{aligned} \tag{A.4}$$

Here, u, v, and w are the velocity components in x, y, and z-directions, respectively, and ρ is the thermodynamic density. By dividing the entire equation by $\Delta x \Delta y \Delta z$, we get

$$\frac{\partial}{\partial t}(\rho_i \theta_i \gamma_v) + \frac{\Delta(\rho_i \theta_i u_i \gamma_x)}{\Delta x} + \frac{\Delta(\rho_i \theta_i v_i \gamma_y)}{\Delta y} + \frac{\Delta(\rho_i \theta_i w_i \gamma_z)}{\Delta z} = \Gamma_i \gamma_v , \tag{A.5}$$

where we define

$$\frac{\Delta \phi}{\Delta x_j} = \frac{\left(\phi_{x_j + \frac{\Delta x_j}{2}} - \phi_{x_j - \frac{\Delta x_j}{2}} \right)}{\Delta x_j} . \tag{A.6}$$

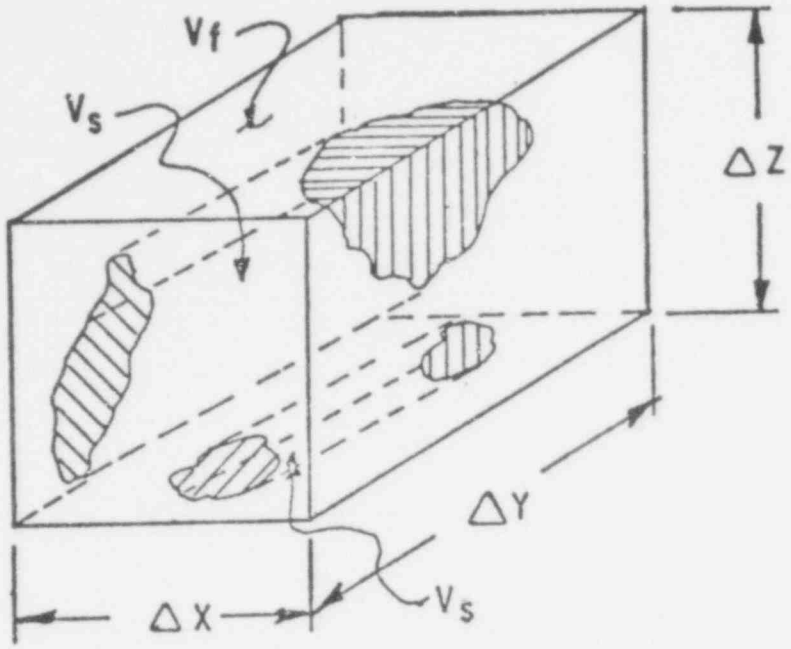

Fig. A-1. Elementary control volume partially occupied by solid objects.

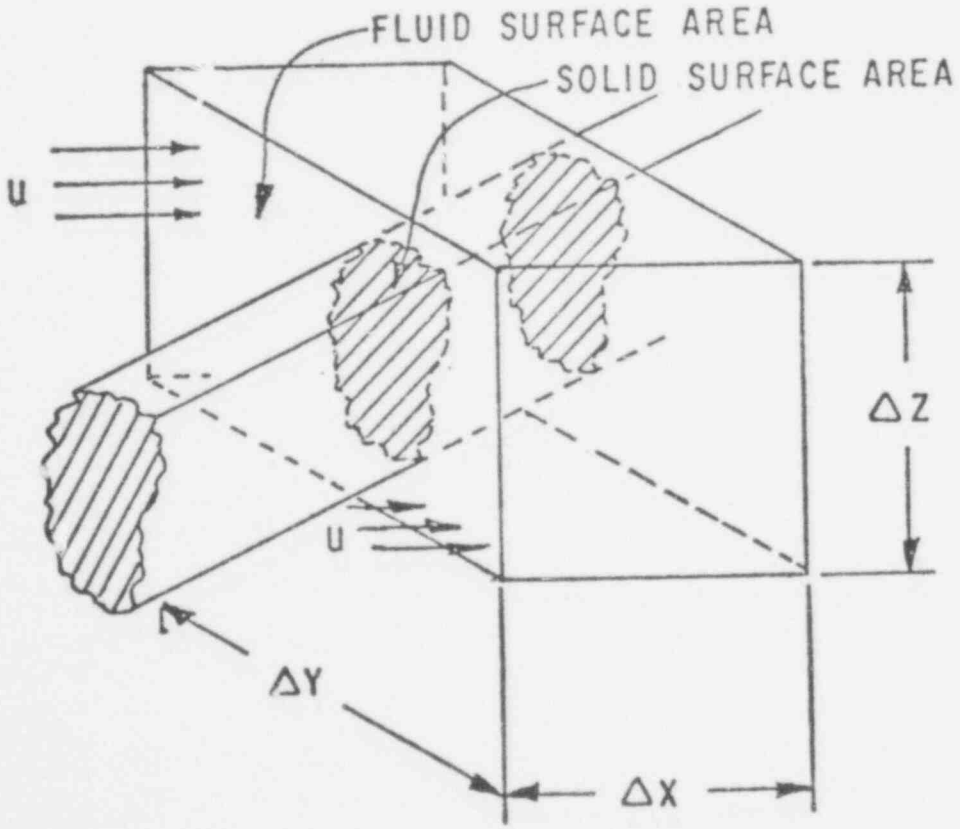

Fig. A-2. Control volume showing surface permeability in x-direction.

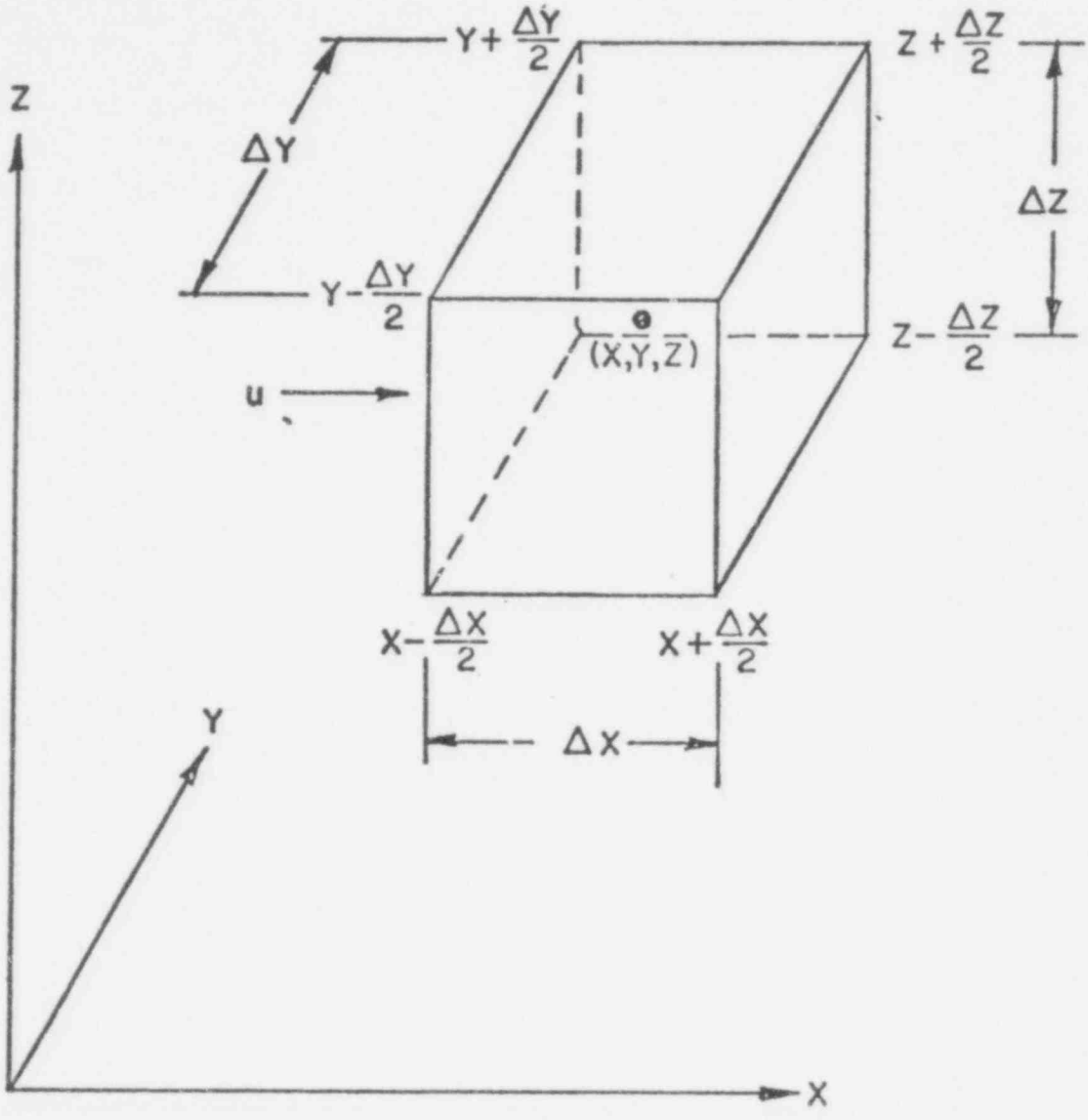

Fig. A-3. Elementary control volume.

A.5 Momentum Equation

For a two-phase fluid flowing in a space which is partially occupied by solid objects, we have to account for two additional resistances in the momentum equation. These are due to (1) the interaction between two phases, and (2) the interaction between fluid and solid surfaces.

The interaction between two phases is a very complex and not well understood phenomenon. At present, there are several mathematical models in existence in the literature postulating the interaction between two phases. In the present development, we adopt the model which assumes that the interfacial resistance can be expressed by the following relation:

Resistance per unit fluid volume = K (Difference in phase velocities). (A.7)

Hence, the total interfacial resistance in x-direction for phase i for control volume as shown in Fig. A.3 is

$$\text{Interfacial resistance} = K_x \gamma_v \Delta x \Delta y \Delta z (u_2 - u_1). \tag{A.8}$$

Here, K_x is the interfacial friction coefficient, which depends on Reynolds number, void fraction, phase velocity difference, and the shapes and sizes of dispersed phase (bubbles/droplets). A high value of K represents that both phases are moving at the same velocity.

In regard to the interaction between fluid and solid surfaces, we assume that the solid objects in a flow domain produce distributed resistances to flow, and that we can express these distributed resistances through source (sink) terms in the momentum equation. With these remarks about interactions and with the definitions of porosities and $\Delta\Phi/\Delta x_j$ (Eq. A.6), we can now derive the momentum equation.

Consider the momentum balance in x-direction for phase 1 and for a control volume as shown in Fig. A.3. First, we describe each term:

Rate of Change of Momentum

$$\frac{\partial}{\partial t} (\rho_1 \theta_1 \gamma_v u_1 \Delta x \Delta y \Delta x) \tag{A.9}$$

Convective Flux

$$-\Delta x \Delta y \Delta z \left[\frac{\Delta(\rho_1 \theta_1 \gamma_x u_1^2)}{\Delta x} + \frac{\Delta(\rho_1 \theta_1 \gamma_y u_1 v_1)}{\Delta y} + \frac{\Delta(\rho_1 \theta_1 \gamma_z u_1 w_1)}{\Delta z} \right] \tag{A.10}$$

Pressure and Body Force (Fig. A.4; Fig. A.5)

$$\Delta x \Delta y \Delta z \left[- \frac{\Delta(p)}{\Delta x} \theta_1 \gamma_v + \rho_1 \theta_1 \gamma_v g_x \right] \tag{A.11}$$

The pressure forces are usually considered surface forces. However, in this case, it is the pressure gradient force which acts on a unit volume of the fluid. Hence we regard the pressure force as a body force term in the present derivation.

Viscous Transfer (Fig. A.5)

$$\Delta x\Delta y\Delta z \left[\frac{\Delta(\tau_{xx}\gamma_x\theta_1)}{\Delta x} + \frac{\Delta(\tau_{xy}\gamma_y\theta_1)}{\Delta y} + \frac{\Delta(\tau_{xz}\gamma_z\theta_1)}{\Delta z}\right] \tag{A.12}$$

Here τ_{xx}, τ_{xy}, and τ_{xz} are the viscous stresses acting on the surfaces of the control volume.

Distributed Resistance (Fig. A.4)

$$\Delta x\Delta y\Delta z\ [R_x], \tag{A.13}$$

where R_x is the distributed frictional resistance per unit volume in x-direction.

Interfacial Force (Fig. A.4)

$$\Delta x\Delta y\Delta z\ \{\gamma_v K_x(u_2-u_1)\} \tag{A.14}$$

We now write the momentum balance for x-direction:

$$\frac{\partial}{\partial t}(\rho_1\theta_1\gamma_v u_1) + \frac{\Delta(\rho_1\theta_1\gamma_x u_1^2)}{\Delta x} + \frac{\Delta(\rho_1\theta_1\gamma_y u_1 v_1)}{\Delta y} + \frac{\Delta(\rho_1\theta_1\gamma_z u_1 w_1)}{\Delta z} =$$

$$\gamma_v K_x(u_2 - u_1) - \theta_1\gamma_v\frac{\Delta(p)}{\Delta x} + \rho_1\theta_1\gamma_v g_x - R_x + \frac{\Delta(\tau_{xx}\gamma_x)}{\Delta x} + \frac{\Delta(\tau_{xy}\gamma_y)}{\Delta y} + \frac{\Delta(\tau_{xz}\gamma_z)}{\Delta z} \quad . \tag{A.15}$$

Equations are similar for other directions.

Energy Equation

As in the previous section for momentum balance, we must account for two additional interactions; the interactions between the phases, and the interactions between fluids and solid surfaces. Therefore, we adopt the same mathematical models to describe these interactions. Thus we define:

Heat transfer between phases per unit fluid volume = R (Temperature difference between phases), (A.16)

and

Heat transfer between fluid and solid surfaces per unit volume = Q_s. (A.17)

With these definitions, we can now write all terms of the energy equation for phase 1.

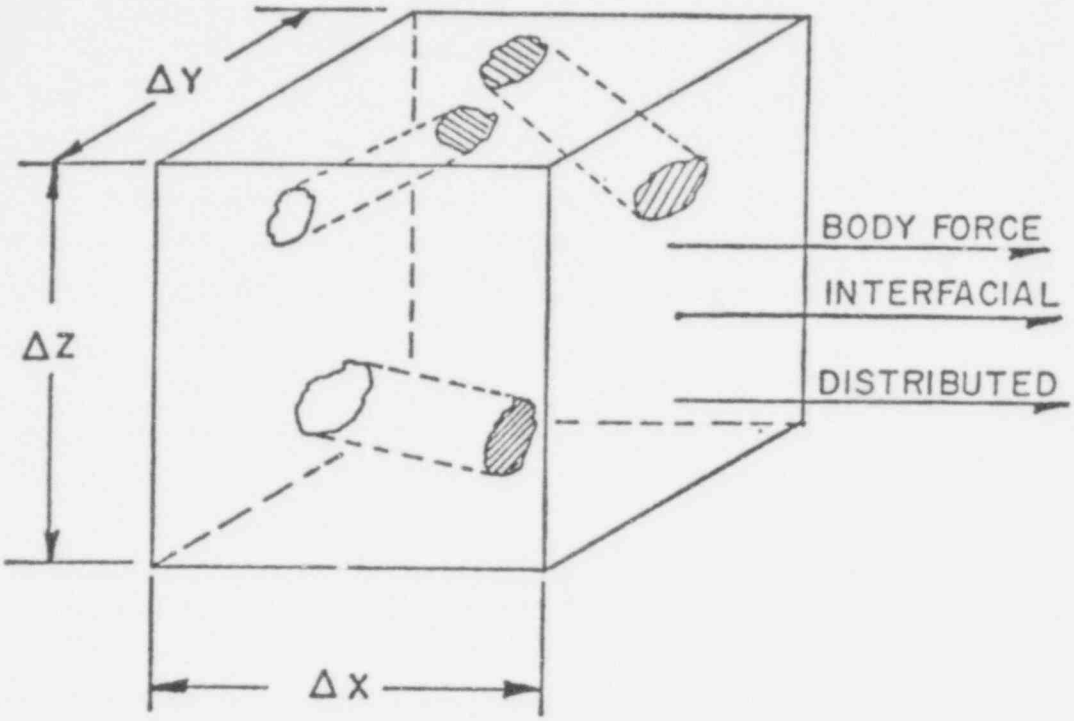

Body Force: $(\Delta x \Delta y \Delta z \gamma_v)\ \rho g_x$

Interfacial: $(\Delta x \Delta y \Delta z \gamma_v)\ K_x(u_2 - u_1)$

Distributed: $\iint (\tau_{xx_s} dA_{x_s} + \tau_{xy_s} dA_{y_s} + \tau_{xz_s} dA_{z_s}) = \Delta x \Delta y \Delta z R_x$
Surface Area of Distributed Solids

Subscript s: Solid Surface Inside the Control Volume

Fig. A-4. Volumetric forces.

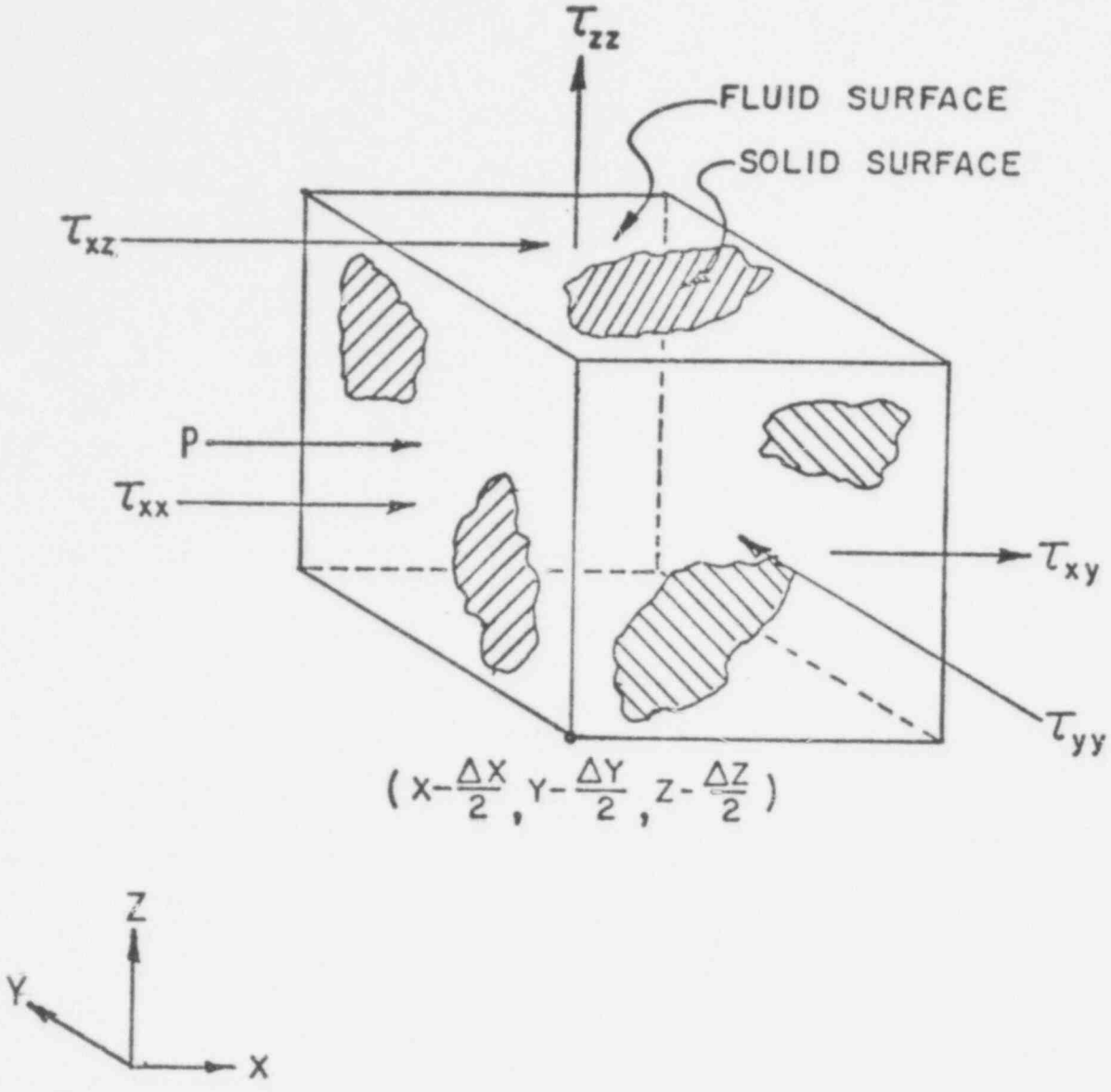

Fig. A-5. Surface forces.

Rate of Change of Energy

$$\Delta x\Delta y\Delta z\ [\frac{\partial}{\partial t}(\rho_1\theta_1\gamma_v E_1)] = \Delta x\Delta y\Delta z\ [\frac{\partial}{\partial t}(\rho_1\theta_1\gamma_v(H_1-p/\rho_1))]$$

$$= \Delta x\Delta y\Delta z \left[\frac{\partial}{\partial t}(\rho_1\theta_1\gamma_v H_1) - \frac{\partial}{\partial t}(C_1\gamma_v p)\right] \qquad (A.18)$$

Here, E is the sum of internal and kinetic energy per unit mass, and H = E + p/p is the sum of enthalpy and kinetic energy per unit mass.

Note that γ_v is not a function of time, and can be eliminated from the differential with respect to time.

Convective Flux

$$-\Delta x\Delta y\Delta z \left[\frac{\Delta(\rho_1\theta_1 u_1\gamma_x E_1)}{\Delta x} + \frac{\Delta(\rho_1\theta_1 v_1\gamma_y E_1)}{\Delta y} + \frac{\Delta(\rho_1\theta_1 w_1\gamma_z E_1)}{\Delta z}\right], \qquad (A.19)$$

which we rewrite in terms of enthalpy and pressure:

$$-\left\{\left[\frac{\Delta(\rho_1\theta_1 u_1\gamma_x H_1)}{\Delta x} + \frac{\Delta(\rho_1\theta_1 v_1\gamma_y H_1)}{\Delta y} + \frac{\Delta(\rho_1\theta_1 w_1\gamma_z H_1)}{\Delta z}\right]\right.$$

$$\left.-\left[\frac{\Delta(\theta_1 u_1\gamma_x p)}{\Delta x} + \frac{\Delta(\theta_1 v_1\gamma_y p)}{\Delta y} + \frac{\Delta(\theta_1 w_1\gamma_z p)}{\Delta z}\right]\right\} \Delta x\Delta y\Delta z\ . \qquad (A.20)$$

Pressure Work

$$-\left[\frac{\Delta(\theta_1 u_1\gamma_x p)}{\Delta x} + \frac{\Delta(\theta_1 v_1\gamma_y p)}{\Delta y} + \frac{\Delta(\theta_1 w_1\gamma_z p)}{\Delta z}\right] \Delta x\Delta y\Delta z \qquad (A.21)$$

Work Due to Viscous Forces

$$\Delta x\Delta y\Delta z \left\{\frac{\Delta[\theta_1\gamma_x(\tau_{xx}u_1+\tau_{xy}v_1+\tau_{xz}w_1)]}{\Delta x} + \frac{\Delta[\theta_1\gamma_y(\tau_{xy}u_1+\tau_{yy}v_1+\tau_{yz}w_1)]}{\Delta y}\right.$$

$$\left. + \frac{\Delta[\theta_1\gamma_z(\tau_{xz}u_1+\tau_{yz}v_1+\tau_{zz}w_1)]}{\Delta z}\right\} \qquad (A.22)$$

Work Due to Body Force

$$\Delta x\Delta y\Delta z\ [\rho_1\theta_1\gamma_v(g_x u_1 + g_y v_1 + g_z w_1)] \qquad (A.23)$$

Diffusion

$$-\Delta x\Delta y\Delta z \left[\frac{\Delta(\theta_1\gamma_x q_x)}{\Delta x} + \frac{\Delta(\theta_1\gamma_y q_y)}{\Delta y} + \frac{\Delta(\theta_1\gamma_z q_z)}{\Delta z}\right] \qquad (A.24)$$

Here, q is the conductive heat transfer per unit surface area, which can be expressed in terms of temperature gradient by

$$\Delta x\Delta y\Delta z \left[\frac{\Delta(\theta_1\gamma_x k_1\frac{\partial T_1}{\partial x})}{\Delta x} + \frac{\Delta(\theta_1\gamma_y k_1\frac{\partial T_1}{\partial y})}{\Delta y} + \frac{\Delta(\theta_1\gamma_z k_1\frac{\partial T_1}{\partial z})}{\Delta z}\right]. \qquad (A.25)$$

Interactions and Heat Source

$$\Delta x\Delta y\Delta z \left[\underbrace{\dot{Q}_{1s}}_{\substack{\text{Interaction between}\\ \text{fluid and solid surface}}} + \underbrace{\gamma_v \dot{q}_1}_{\text{Heat Source}} + \underbrace{\gamma_v R(T_2 - T_1)}_{\substack{\text{Interaction between}\\ \text{two phases}}} \right] . \qquad (A.26)$$

Here, $\dot{q}$ is the heat source per unit fluid volume.

We now write the complete energy equation: (Note that the pressure term in the convective flux cancels out the pressure work term.)

$$\frac{\partial}{\partial t}(\rho_1\theta_1\gamma_v H_1) + \left[\frac{\Delta(\rho_1\theta_1 U_1\gamma_x H_1)}{\Delta x} + \frac{\Delta(\rho_1\theta_1 v_1\gamma_y H_1)}{\Delta y} + \frac{\Delta(\rho_1\theta_1 w_1\gamma_z H_1)}{\Delta z}\right]$$

$$= \gamma_V \frac{\partial}{\partial t}(\theta_1 p) + \frac{\Delta\left[\theta_1\gamma_x(\tau_{xx}u_1 + \tau_{xy}v_1 + \tau_{xz}w_1)\right]}{\Delta x} + \frac{\Delta\left[\theta_1\gamma_y(\tau_{xy}u_1 + \tau_{yy}v_1 + \tau_{yz}w_1)\right]}{\Delta y}$$

$$+ \frac{\Delta\left[\theta_1\gamma_z(\tau_{xz}u_1 + \tau_{yz}v_1 + \tau_{zz}w_1)\right]}{\Delta z} + \left[\rho_1\theta_1\gamma_v(g_x u_1 + g_y v_1 + g_z w_1)\right]$$

$$+ \left[\frac{\Delta\left(\theta_1\gamma_x k_1 \frac{\partial T_1}{\partial x}\right)}{\Delta x} + \frac{\Delta\left(\theta_1\gamma_y k_1 \frac{\partial T_1}{\partial y}\right)}{\Delta y} + \frac{\Delta\left(\theta_1\gamma_z k_1 \frac{\partial T_1}{\partial z}\right)}{\Delta z}\right]$$

$$+ \left[\dot{Q}_{1s} + \gamma_v\dot{q}_1 + \gamma_v R(T_2 - T_1)\right] - \left(R_x u_1 + R_y v_1 + R_z w_1\right) . \qquad (A.27)$$

Here the last term is the source due to distributed resistance. If the kinetic energy is negligible, we can replace the stagnation enthalpy H by the thermodynamic enthalpy h. Alternatively, we can derive the equation for enthalpy by subtracting the kinetic energy terms, making use of the momentum equation. We then get:

$$\frac{\partial}{\partial t}(\rho_1\theta_1\gamma_v h_1) + \left[\frac{\Delta\left(\rho_1\theta_1 u_1\gamma_x h_1\right)}{\Delta x} + \frac{\Delta\left(\rho_1\theta_1 v_1\gamma_y h_1\right)}{\Delta y} + \frac{\Delta\left(\rho_1\theta_1 w_1\gamma_z h_1\right)}{\Delta z}\right]$$

$$= \gamma_v \frac{dp}{dt} + \theta_1\gamma_x\left[\tau_{xx}\left(\frac{\Delta u_1}{\Delta x}\right) + \tau_{xy}\left(\frac{\Delta v_1}{\Delta x}\right) + \tau_{xz}\left(\frac{\Delta w_1}{\Delta x}\right)\right]$$

$$+ \theta_1\gamma_y\left[\tau_{xy}\left(\frac{\Delta u_1}{\Delta y}\right) + \tau_{yy}\left(\frac{\Delta v_1}{\Delta y}\right) + \tau_{zy}\left(\frac{\Delta w_1}{\Delta y}\right)\right]$$

$$+ \theta_1\gamma_z\left[\tau_{xz}\left(\frac{\Delta u_1}{\Delta z}\right) + \tau_{yz}\left(\frac{\Delta v_1}{\Delta z}\right) + \tau_{zz}\left(\frac{\Delta w_1}{\Delta z}\right)\right]$$

$$+\left[\frac{\Delta\left(\theta_1\gamma_x k_1 \frac{\partial T_1}{\partial x}\right)}{\Delta x} + \frac{\Delta\left(\theta_1\gamma_y k_1 \frac{\partial T_1}{\partial y}\right)}{\Delta y} + \frac{\Delta\left(\theta_1\gamma_z k_1 \frac{\partial T_1}{\partial z}\right)}{\Delta z}\right]$$

$$+\left[\dot{Q}_{1s} + \gamma_v \dot{q}_1 + \gamma_v R\left(T_2 - T_1\right)\right]. \qquad \text{(A.28)}$$

References

1. W. T. Sha and S. L. Soo, "Multidomain and Multiphase Fluid Mechanics," ANL-CT-77-3 (Mar 1977).

2. W. T. Sha, H. M. Domanus, R. C. Schmitt, J. J. Oras, and E. I. H. Lin, "COMMIX-1: A Three-Dimensional, Transient, Single-Phase Component Computer Program for Thermal-Hydraulic Analysis", NUREG-0415; ANL-77-96 (Sept 1978).

3. F. H. Harlow and A. A. Amsden, "Flow of Interpenetrating Material Phases," J. Comput. Phys. 18, 440-464 (1975)

4. W. C. Rivard and M. D. Torrey, "K-Fix: A Computer Program for Transient, Two-Dimensional, Two-Fluid Flow," LA-NUREG-6623, (1977)

5. H. Schweickert, "Investigation of Phenomena in a Multiply Subdivided Containment Following Rupture of a Cooling Pipe in a Water-Cooled Reactor," Technical Report BFR 50-32-C12-1, Kraftwerk Union, Germany (1956).

DISTRIBUTION

A. Lillie
Atomics International
8900 DeSoto Avenue
Canoga Park, California 91303

G. Grant
Babcock and Wilcox Company
Breeder Reactor Development Program
20 S. VanBuren Street
Barberton, Ohio 44203

D. Dietrich
Combustion Engineering, Inc.
1000 Prospect Hill Road
Windsor, Connecticut 06095

C. L. Storrs, Director
FBR Development
C-E Power Systems
Combustion Engineering, Inc.
1000 Prospect Hill Road
Windsor, Connecticut 06095

P. Magee
General Electric Company
310 DeGuigne Drive
Sunnyvale, California 94086

D. Bongaards
Westinghouse Electric Corporation
6001 S. Westshore Boulevard
Tampa, Florida 33616

W. J. Severson
Advanced Reactors Division
Westinghouse Electric Corporation
P. O. Box 158
Madison, Pennsylvania 15663

Dr. A. A. Bishop
Chemical/Petroleum Engineering Department
1259 Benedum Hall
University of Pittsburgh
Pittsburgh, Pennsylvania 15261

Professor B. T. Chao
Department of Mechanical Engineering
University of Illinois
Urbana, Illinois 61801

Dr. Neil E. Todreas
Department of Nuclear Engineering
Massachusetts Institute of Technology
138 Albany Street
Cambridge, Massachusetts 02139

Mr. E. H. Novendstern, Manager
Thermal and Hydraulic Analysis
Westinghouse Advanced Reactor Division
P. O. Box 158
Madison, Pennsylvania 15663

Mr. R. Markley
Westinghouse Electric Corporation
Advanced Reactors Division
Waltz Mill Site
P. O. Box 158
Madison, Pennsylvania 15663

Professor S. L. Soo
Department of Mech. & Industrial Engr.
144 Mechanical Engineering Building
University of Illinois
Urbana, Illinois 61801

Professor Brian E. Launder
University of California
Davis, California 95616

Professor John C. Slattery
Chemical Engineering Department
The Technological Institute
Northwestern University
Evanston, Illinois 60201

Professor John C. Chen
Department of Mechanical Eng. & Mechanics
Lehigh University
Bethlehem, Pennsylvania 18015

DISTRIBUTION

Professor M. Doria
Valparaiso University
Valparaiso, Indiana

Professor S. H. Chan
College of Engineering and Applied Science
University of Wisconsin-Milwaukee
Milwaukee, Wisconsin 53201

Professor D. H. Schultz
Department of Mathematics
University of Wisconsin-Milwaukee
Milwaukee, Wisconsin 53201

Professor A. A. Szewczyk
Department of Aerospace and Mech. Engr.
University of Notre Dame
Notre Dame, Indiana 46556

DISTRIBUTION

OTD

J. A. Kyger

CT

Bldg. 308

R. S. Zeno
P. R. Huebotter
A. R. Brunsvold
Y. S. Cha
B. Chen
J. DePaz
H. M. Domanus
P. A. Howard
K. A. Kasza
P. Kehler
J. L. Krazinski (5)
E. I. H. Lin
J. J. Lorenz
J. T. Madell
C. C. Miao (5)
J. J. Oras
A. W. Schaeper
R. C. Schmitt
W. T. Sha (40)
V. L. Shah (10)
W. R. Simmons
C. C. Stone
S. P. Vanka
C. I. Yang
D. Yung

Bldg. 335

G. S. Rosenberg
R. A. Valentin
M. W. Wambsganss
S. S. Chen
Y. W. Shin

RAS

W. L. Chen
D. H. Cho
H. K. Fauske
M. Ishii
T. M. Kuzah
R. K. Lo
W. W. Marr
Y. W. Chang

EBR-II

P. R. Betten
L. K. Chang
E. E. Feldman
R. M. Singer

AMD

G. Leaf